Naval Research Laboratory

Washington, DC 20375-5000

NRL Memorandum Report 6554

Solution of the Boltzmann Equation Using an Energy Group Method

D. COLOMBANT AND M. LAMPE

Beam Physics Branch
Plasma Physics Division

October 2, 1989

UNCLASSIFIED
SECURITY CLASSIFICATION OF THIS PAGE

REPORT DOCUMENTATION PAGE

Form Approved
OMB No. 0704-0188

1a. REPORT SECURITY CLASSIFICATION UNCLASSIFIED	1b. RESTRICTIVE MARKINGS
2a. SECURITY CLASSIFICATION AUTHORITY	3. DISTRIBUTION / AVAILABILITY OF REPORT Approved for public release; distribution unlimited.
2b. DECLASSIFICATION / DOWNGRADING SCHEDULE	
4. PERFORMING ORGANIZATION REPORT NUMBER(S) NRL Memorandum Report 6554	5. MONITORING ORGANIZATION REPORT NUMBER(S)
6a. NAME OF PERFORMING ORGANIZATION Naval Research Laboratory 6b. OFFICE SYMBOL (If applicable) Code 4790	7a. NAME OF MONITORING ORGANIZATION
6c. ADDRESS (City, State, and ZIP Code) Washington, DC 20375-5000	7b. ADDRESS (City, State, and ZIP Code)
8a. NAME OF FUNDING / SPONSORING ORGANIZATION DARPA 8b. OFFICE SYMBOL (If applicable)	9. PROCUREMENT INSTRUMENT IDENTIFICATION NUMBER
8c. ADDRESS (City, State, and ZIP Code) Arlington, VA 22209	10. SOURCE OF FUNDING NUMBERS PROGRAM ELEMENT NO: 62707E PROJECT NO: ARPA 4395,A80 TASK NO: WORK UNIT ACCESSION NO: DN680-415

11. TITLE (Include Security Classification)
Solution of the Boltzmann Equation Using an Energy Group Method

12. PERSONAL AUTHOR(S)
Colombant, D. and Lampe, M.

13a. TYPE OF REPORT	13b. TIME COVERED	14. DATE OF REPORT (Year, Month, Day)	15. PAGE COUNT
Interim	FROM _____ TO _____	1989 October 2	45

16. SUPPLEMENTARY NOTATION

17. COSATI CODES			18. SUBJECT TERMS (Continue on reverse if necessary and identify by block number)
FIELD	GROUP	SUB-GROUP	Boltzmann equation Secondary electrons

19. ABSTRACT (Continue on reverse if necessary and identify by block number)

We have developed and explored a method for solving the nonlocal linear Boltzmann equation by taking velocity moments while retaining the kinetic energy as an independent variable. The six-dimensional Boltzmann equation is reduced to a set of four-dimensional equations that formally resemble fluid equations. We have implemented a numerical code for solving these equations. We have tried a number of schemes for closing the hierarchy of moment equations. The validity and accuracy of the method has been tested by running a number of test problems for which exact solutions of the Boltzmann equation are available. These test problems all involve one-dimensional collision-free, free-streaming, which is trivial from the viewpoint of the Boltzmann equation, but which poses a severe test to the model, whose accuracy is improved by the smoothing effects of collisions. Satisfactory closure schemes have been found for each of the test problems, but it appears that the closure methods may have to become increasingly elaborate as more complicated situations are considered, and thus it is still not clear whether the method will be practical in treating real applications.

20. DISTRIBUTION / AVAILABILITY OF ABSTRACT	21. ABSTRACT SECURITY CLASSIFICATION
☒ UNCLASSIFIED/UNLIMITED ☐ SAME AS RPT ☐ DTIC USERS	UNCLASSIFIED
22a. NAME OF RESPONSIBLE INDIVIDUAL D. Colombant	22b. TELEPHONE (Include Area Code) (202) 404-7721 22c. OFFICE SYMBOL Code 4790

DD Form 1473, JUN 86 *Previous editions are obsolete.*
S/N 0102-LF-014-6603

SECURITY CLASSIFICATION OF THIS PAGE
UNCLASSIFIED

CONTENTS

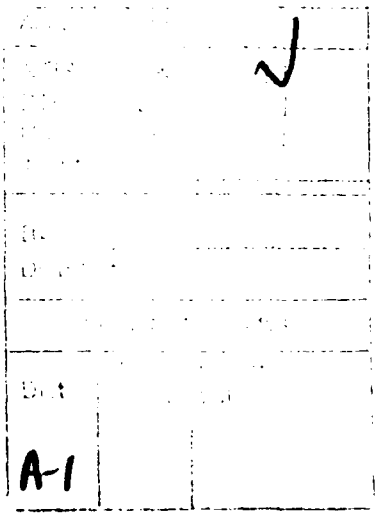

SOLUTION OF THE BOLTZMANN EQUATION USING AN ENERGY GROUP METHOD

I. Introduction

In certain regimes of beam propagation, it has been shown that high energy plasma electrons whose mean free path is long (but not infinite) may play an important role. Such electrons may be delta rays (beam-generated secondaries) or thermal electrons accelerated by large electric fields. Since high energy electrons produce nonlocal transport, they are not correctly represented by eitner Ohm's conductivity law or by fluid equations. The correct representation is the linear Boltzmann equation - linear because electron-electron collisions may be neglected but collisions of electrons with nearly-stationary ions must be included. Needless to say, the linear Boltzmann equation is also the central equation in many other scientific disciplines. However, the Boltzmann equation is a six-dimensional integro-differential equation in phase-space (plus time) and can only be solved by approximate methods. Many attempts have been made at solving that equation and various approximations have been made. Within the beam propagation context, analysis of nonlocal transport by high energy plasma electrons has depended primarily on Monte Carlo[1] and particle simulation techniques,[2] which are strongly constrained by computer time and/or storage; or fluid approximations,[3] which are very approximate; or spherical harmonic expansions of the Boltzmann equation.[4,5] The latter technique has been highly successful in deducing atomic and molecular properties from swarm experiments, and it has been argued that even two-term spherical harmonic expansions are valid even for highly anisotropic cases.[5] Indeed there are problems and particular cross-sections for which two-term expansions are accurate, but, in general, they are very inaccurate, even divergent, in the anisotropic limit of nearly collisionless streaming.

Manuscript approved August 9, 1989.

In this report, we describe and explore a new technique[6] which is based on choosing the energy of particles as an independent variable. This selection is suggested by the strong dependence of high energy electron mean free paths and/or scattering kernels on the electron speed. Before applying this method to full scale problems, we have applied it to various collisionless test problems ranging from the simplest (force-free, free-expanding electrons), to more complicated ones like shear flow in one dimension. These test problems have two characteristics:

- They allow a comparison with exact analytical solutions which can be obtained directly from the original linear Boltzmann equation.

- Because these tests are collisionless, they constitute severe tests of the numerical solution since no physical smoothing of the solution is provided in the equations.

The outline of this report is the following. In the first section, we illustrate problems with some of the previous methods used to solve the linear Boltzmann equation. In the second section, we present the equations and the approximation we make to solve these equations. In the third part, the numerical scheme is presented. In the ensuing sections, we report successively on the following collisionless test problems: free-streaming, free-streaming in the direction parallel to the flow and perpendicular to the flow and finally shear flow. A review of these results and recommendations for future work will then follow in the final section.

II. Example of Problems Associated with Approximations in Solving Boltzmann Equation

In this section, we consider a simple problem, i.e., collisionless steady-state, one-dimensional cold flow of electrons subject to a constant electric field E_z. In this case, the Boltzmann equation reduces to

$$v_z \frac{\partial f}{\partial z} + \frac{qE}{m} \frac{\partial f}{\partial v_z} = 0, \tag{1}$$

with the boundary conditions

$$f(z = 0, \underset{\sim}{v}) = \delta(v_x)\delta(v_y)\delta(v_z - v_o), \tag{2a}$$

$$f(z \to \infty, \underset{\sim}{v}) = 0 \text{ for } v_z < 0. \tag{2b}$$

We assume that $qE > 0$, so that electrons are accelerated toward $z = \infty$. The exact solution is

$$f(z, \underset{\sim}{v}) = \delta(v_x)\delta(v_y)\delta\left[v_z - \left(v_o^2 + \frac{2qE_z}{m}\right)^{1/2}\right](v_o/v_z)\Theta(v_z), \tag{3}$$

where Θ is the step function. Taking moments, we find that the density $N(z)$ and fluid velocity $U_z(z)$ are given by the first column of Table 1, wherein V is defined by $V^2 = U^2 + 2qEz/m$.

Table 1

	Exact	2-Polynomial	4-Polynomial
N	$N_o \frac{U_o}{v}$	$N_o \frac{v}{U_o}$	$N_o \frac{v}{U_o}\left(1 + \frac{10qE_z}{mU_o^2}\right)$
U_z	v	$\frac{U_o^2}{v}$	$\frac{U_o^2}{v}\left(1 + \frac{10qE_z}{mU_o^2}\right)^{-1}$
NU_z	N_oU_o	N_oU_o	N_oU_o

We have also worked out the values of these macroscopic quantities by solving the two-polynomial and four-polynomial expansions of the Boltzmann

equation. It is seen in Table 1 that NU_z is given exactly by the polynomial expansions, but that with increasing z, the two-polynomial expansion shows N increasing monotonically to infinity whereas the exact solution has N decreasing monotonically to zero, and conversely for U_z. Thus, the polynomial solution could hardly be more wrong. Even more disturbing, the four polynomial expansion worsens the error. (Incidentally, if an initial value spatially-uniform problem were solved, rather than a steady state problem, N would be given correctly by the polynomial approximations but U_z and NU_z would be totally incorrect.) The error can be traced to the fact that the few-polynomial expansions assume near-isotropy, and, therefore, incorrectly heat the transverse dimensions. Equally disturbing is the absence of nonlinear conductive terms in the polynomial formulation.

The method we propose here is an alternative type of expansion which also focuses on density and current, the quantities of principal interest, and also retains energy as an independent variable, but which becomes exact in both the near isotropic limit and the cold fluid nearly collisionless limit.

III. Equations

The method starts with the linear Boltzmann equation

$$\frac{\partial f}{\partial t} + \underset{\sim}{v} \cdot \frac{\partial f}{\partial \underset{\sim}{x}} + \frac{1}{m}\left[q\underset{\sim}{E}(\underset{\sim}{x},t) + q\underset{\sim}{v} \times \underset{\sim}{B}(\underset{\sim}{x},t)\right] \cdot \frac{\partial f}{\partial \underset{\sim}{v}} = \int d^3\underset{\sim}{v}' K(\underset{\sim}{v}',\underset{\sim}{v}) f(\underset{\sim}{x}',\underset{\sim}{v}',t), \tag{4}$$

where f is the distribution function in space and velocity and K is the scattering kernel. Now, by taking moments over velocity angles while keeping the speed w, i.e., the kinetic energy, as an independent variable, the Boltzmann equation yields two coupled equations:

$$\frac{\partial n}{\partial t} + \left(\frac{\partial}{\partial \underset{\sim}{x}} + \frac{q\underset{\sim}{E}}{m} \frac{\partial}{\partial w} \frac{1}{w}\right) \cdot n\underset{\sim}{u} = \int_o^\infty dw' \left[n(w')K_o(w,w') - n(w)K_o(w',w)\right], \quad (5a)$$

$$\frac{\partial \underset{\sim}{u}}{\partial t} + \underset{\sim}{u} \cdot \left(\frac{\partial}{\partial \underset{\sim}{x}} + \frac{q\underset{\sim}{E}}{m} \frac{\partial}{\partial w} \frac{1}{w}\right) \underset{\sim}{u} + \frac{1}{m} \left(\frac{\partial}{\partial \underset{\sim}{x}} + \frac{q\underset{\sim}{E}}{m} \frac{\partial}{\partial w} \frac{1}{w}\right) \cdot \underset{\sim}{P}(w) =$$

$$\frac{q}{m} \left(\underset{\sim}{E} + \underset{\sim}{u} \times \underset{\sim}{B}\right) + \int_o^\infty dw' \left[\frac{w}{w'} \frac{n(w')}{n(w)} \underset{\sim}{u}(w')K_1(w',w) - \frac{n(w')}{n(w)} \underset{\sim}{u}(w)K_o(w',w)\right], \quad (5b)$$

where $n(x,t,w)$ is the "microscopic" density of particles with speed w, and u is the mean velocity of the class of electrons with speed w, defined respectively as

$$n(\underset{\sim}{x},t,w) = \int d^3\underset{\sim}{v}\ \delta\ (|\underset{\sim}{v}| - w)\ f\ (\underset{\sim}{x},\underset{\sim}{v},t), \quad (6)$$

$$n(\underset{\sim}{x},t,w)\ \underset{\sim}{u}\ (\underset{\sim}{x},t,w) = \int d^3\underset{\sim}{v}\ \delta\ (|\underset{\sim}{v}| - w)\ \underset{\sim}{v}\ f(\underset{\sim}{x},\underset{\sim}{v},t) \quad (7)$$

$K_o\ (w,w')$ and $K_1\ (w,w')$ are integrated scattering kernels and are defined as

$$K_o\ (w,w') = 2\pi \int_o^\pi d\chi\ \sin\ \chi\ K\ (w,w',\chi) \quad (8)$$

$$K_1\ (w,w') = 2\pi \int_o^\pi d\chi\ \sin\ \chi\ \cos\ \chi\ K\ (w,w',\chi) \quad (9)$$

where χ is the angle between v and v'.

To close the hierarchy of moment equations, one approximation is made: we assume that the microscopic pressure tensor (for particles with speed w)

$$\underset{\sim}{p}(\underset{\sim}{x},t,w) = m \int d^3\underset{\sim}{v}\ \delta\ (|\underset{\sim}{v}| - w)\ \left[\underset{\sim}{v} - \underset{\sim}{u}(w)\right]\left[\underset{\sim}{v} - \underset{\sim}{u}(w)\right] f(\underset{\sim}{v}) \quad (10)$$

can be replaced by an isotropic scalar value

$$p(\underset{\sim}{x},t,w) = \frac{1}{3}\, n(w)\, \left[w^2 - u^2(w)\right] \qquad (11)$$

which is then uniquely specified by the requirement that the particles in question have speed w.

Let us note that this form of the pressure represents exactly the sum of the three diagonal components of p(z,t,w) i.e., it does not mix streaming energy with thermal energy (as do low-order spherical harmonic expansions of the Boltzmann equation, for example). This approximation would appear to be a relatively weak one compared to those that are made in deriving macroscopic fluid approximations; however, we shall see that it does lead to some serious problems. This technique reduces the six-dimensional Boltzmann equation to a pair of four-dimensional equations and a great simplification. We shall concentrate in this report, however, on potential problems and deficiencies, and how we have explored them. In particular, the isotropic-microscopic-pressure assumption is weakest in the completely collisionless limit. In this limit, it is often possible to write down exact solutions of Eq. (4) in closed form in terms of simple integrals over the deterministic orbits. We have thus been able to compare these exact solutions to those of our model. Let us keep in mind that we are discussing a model for the Boltzmann equation, rather than a precision approximation scheme. (Even so, this would be an improvement in the present state-of-the-art.) It is important to note that our real interest is in calculating the macroscopic electron density and current, for use as sources in the field equations; getting these quantities right should be easier than calculating all the microscopic distributions accurately.

Displaced Maxwellian

We may first ask how well Eq. (11) represents p(z,t,w) in simple test cases, like displaced Maxwellian velocity distributions,

$$f(\underset{\sim}{v}) = \exp\left[-(\underset{\sim}{v}-U)^2/v_{th}^2\right]. \tag{12}$$

In Fig. 1, we show the exact values of $p_{||}$ and $p_{\perp}$, obtained by substituting Eq. (12) in Eq. (10), and compare them with the assumed isotropic value in Eq. (11). We note that: (a) $p_{||}$ and $p_{\perp}$ are correct to first order in u/w in the isotropic limit $u \to 0$. (b) $p_{||} \to 0$ and $p_{\perp} \to 0$ in the streaming limit $u \to w$. Here $p \to 0$ as well. However, the exact solution is not isotropic in this limit; rather $p_{||}/p_{\perp} \to 0$. We argue that our representation is adequate, in that $\underset{\sim}{p}$ plays a vanishingly small role in this limit, where the dynamics are dominated by the streaming energy $1/2\ mU^2$. Thus, our approximation is valid to about 20%, where it matters.

Anomalous Cases

It is easy to conceive of particular velocity distributions for which isotropic-microscopic-pressure is not a good approximation. We have already seen one, but in a limit where the value of the pressure is not important. Consider next a counterstreaming case,

$$f(\underset{\sim}{v}) = a\ \delta(\underset{\sim}{v}-U) + b\ \delta(\underset{\sim}{v}-U). \tag{13}$$

Here $p_{\perp} = 0$ and therefore $p_{||}(w) = n(w^2 - u^2)$. On the other hand, consider a distribution which is initially spatially localized to a thin sheet at

$z = 0$ and spreads out through collisionless free-streaming,

$$f(z,v,t=0) = \delta(z)\ \exp(-v^2/v_{th}^2), \tag{14}$$

which gives

$$f(z,v,t) = (z - v_z t) \exp(- v^2/v_{th}^2). \qquad (15)$$

Since v_z is here uniquely specified as a function of z, we have $p_{||} = 0$ and therefore,

$$p_\perp(w) = 1/2\ n\ (w^2 - u^2). \qquad (16)$$

These examples illustrate the point that there is no unique microscopic pressure which can correctly represent all the structure that can evolve in six-dimensional phase space, especially in the collisionless limit. Indeed, other macroscopic models inevitably suffer from the same deficiency: for example, the spherical harmonic expansion of the Boltzmann equation would require an enormous number of polynomials to represent either of the cases described, and this would amount essentially to fully resolving 3-D velocity space. We do not regard this as a fatal flaw in our method, inasmuch as one of our objectives is modest: to calculate the macroscopic density and current to reasonable qualitative accuracy (10-30%). To this end, our assumption has the advantages of simplicity and centrality, i.e., it appears equally likely to err in either direction. We have abandoned earlier attempts to define an anisotropic pressure prescription that is more accurate than Eq. (11) in (for example) the single-streaming limit. Such formulas are inevitably found to be less accurate in other limits, and also sacrifice mathematical simplicity.

Sound Waves

A collisionless field-free gas supports no sound waves. However, Eqs. (5a), (5b) and (11) do support a sound wave, with speed $c_s(w) = (w^2 - u^2)^{1/2}$, within each energy population. When w is integrated out to obtain macroscopic quantities, these waves phase mix and damp away as $\exp(-k^2 v_{th}^2 t^2/12)$ (for the case of a Maxwell-Boltzmann distribution); furthermore, the waves are damped if there are collisions or fields coupling different energy groups.

IV. Numerical Solution

In the case of one spatial dimension, the code is similar in structure to a 2-D time-dependent magnetohydrodynamic code and consists of solving Eqs. (5). There is no energy equation since the pressure is specified in closed form. In a first stage, the code has been implemented in the simplest possible geometry, i.e., cartesian 1-D in space but is 2-D-like because w (i.e., energy) is retained as an independent variable. These two dimensions are not treated similarly numerically; for example, the gridding is linear in space and logarithmic in energy. In collisionless cases and in the absence of electric fields as in the test cases considered in this report, there is no exchange between the different energy groups and each energy group is completely independent of its neighbors. Operator-splitting has been used to treat the two dimensions and since the microscopic densities convect in the same way as fluid densities, Flux-Corrected Transport[7] has been chosen for the convection algorithm. Also, the equations have been recast in conservation form and we note that the equivalent convection velocity in the microscopic velocity equation is

$$\gamma \frac{Eu}{w}, \tag{17}$$

where the symbols have been defined previously and where γ is the relativistic factor.

The important output of the code is not the "microscopic" (i.e., w-dependent) quantities which are carried from time step to time step but rather the macroscopic variables such as the macroscopic density N(z,t) and the average macroscopic velocity V(z,t). (We use capital letters to denote these macroscopic quantities.) These are integrals over w of the microscopic variables n(z,t,w) and u(z,t,w). As mentioned before, it is those macroscopic variables which may, in turn, be used as input into other codes or which can be compared to other fluid-type calculations.

A major difference between this code and a fluid code appears in the time step constraint. In an explicit hydrodynamic code, the Courant time step condition can be written

$$\delta t \leq 0.5 \frac{\delta z}{|v| + c_s} , \tag{18}$$

where v is the fluid velocity and c_s is the speed of sound. As seen before, the sound speed, as derived from the isotropic-microscopic-pressure, is equal to

$$\frac{\partial[\rho(w^2-u^2)]}{\partial\rho}^{1/2} = (w^2-u^2)^{1/2} . \tag{19}$$

We see that the speed of sound is a function of the energy group and has a maximum for each group. So, as the energy of the group increases, the time step decreases. If there is a need to include very high energy groups in a calculation, the time step may become very small Since the higher energy groups contain fewer particles, we would be in a situation where the regions of smaller densities would control the time step. This situation

is clearly undesirable numerically and moreover, this time step restriction is not physical in origin since, for a collisionless fluid, there is no true sound speed. The situation arises from the approximate (isotropic) expression used for the microscopic pressure.

Typically, there are many fewer high-energy particles, and these particles have longer mean free paths and thus have a coarser spatial structure. Therefore, a variable space gridding has been devised and implemented for these groups of particles to speed up the calculations. The principle behind this variable gridding is the following: above a predetermined velocity u_c not to exceed twice the thermal velocity, the number of points in the spatial dimension is divided by two. For groups with speed greater than 2 u_c, the number of grid points is divided by two once more and so on. In this fashion, the overall time step criterion is applied to the velocity u_c which is of the order of the thermal velocity and which is much smaller than the largest velocity in the calculation. The total number of grid points in the lowest energy group does not necessarily have to be a power of two since the last spatial point can be dropped out of the next regridding. There is a limit to the number of divisions by two which can be accomplished practically since we must be left in the end with at least half a dozen grid points or so for the highest energy group. Because of that consideration, the time step may not be controlled by the lowest energy group but still by the highest one on a much coarser grid, however.

Several comments can be made about this approach. This technique can easily be extended to multi-spatial dimensions and in the case of two spatial dimensions, for example, the cell becomes 4 times larger (a factor of two in each direction) and in 3-D, the cell becomes 8 times larger at each regridding. This technique also requires a repacking of the arrays in

energy space. This repacking can be done once at the beginning of the calculation and has to be unfolded at each reconstruction of the macroscopic variables, namely for every time step when output is desired. That unfolding requires interpolations. Also, if there are particle exchanges between energy groups (when collisions or electric fields are present), care must be applied since spatial resolution for adjacent energy groups may differ by a factor of two.

Finally, instead of increasing the spatial grid for the higher energy groups, the time evolution of these groups could have been computed on a shorter time scale, basically subcycling the calculation for these groups. It is easy to see that such a procedure would involve many more calculations than the approach described above.

V. Test Problems

1. Force-free free-streaming Maxwellian distribution

In a first series of tests, we have looked at the collisionless case in which the electron distribution is initialized as a thin (but not infinitely thin) sheet in space with no initial mean velocity around a Maxwellian velocity distribution. The initial distribution function is simply expressed as

$$f(z,v,0) = \exp\left(-\frac{z^2}{\Delta^2}\right) \exp\left(-\frac{v^2}{v_{th}^2}\right) \tag{20}$$

The solution for f at all times is given by:

$$f(z,v,t) = \exp\left[-\frac{\left(z-v_z t\right)^2}{\Delta^2}\right] \exp\left(-\frac{v^2}{v_{th}^2}\right) \tag{21}$$

To implement the present model for any given problem, the initial microscopic density and velocity $n(z,0,w)$ and $u(z,0,w)$ have to be calculated from $f(z,v,0)$. The analytical solutions for $n(z,t,w)$ and $u(z,t,w)$ are then calculated by taking integrals over v and compared to the solutions of the model Eqs. (5). In fact, these steps represent a significant amount of algebra and since these manipulations do not constitute the main goals of this study, they will not be presented in detail here. For the very simple example under consideration, even the pressure, as defined in Eq. 11, can be computed exactly in terms of a simple integral:

$$p(z,t,w) = n\left(\frac{z^2}{t^2} - u_z^2(w)\right) + \frac{w\Delta}{\pi v_{th}^3 t^3}\exp\left(-\frac{w^2}{v_{th}^2}\right)\left\{(wt-z)\exp\left[-\left(\frac{wt-z}{\Delta}\right)^2\right]\right.$$

$$\left. + (z-wt)\exp\left[-\left(\frac{wt+z}{\Delta}\right)^2\right]\right\} + \frac{w\Delta^2 e^{-w^2/v_{th}^2}}{\pi v_{th}^3 t^3}\int_{\frac{-wt-z}{\Delta}}^{\frac{wt-z}{\Delta}} e^{-z'^2}dz' \qquad (22)$$

Figures 2 and 3 show $n(z,t,w)$ and $u(z,t,w)$ for two values of w ($0.6\ v_{th}$ and $1.6\ v_{th}$) at $t = 2.96$ ns for $\Delta = 10$ dx where dx is the spatial grid step. For most of the test problems, we have chosen dx = 0.1 cm, $v_{th} = 10^8$ cm/s, the total length of the grid of the order of 2 cm (thus, a perturbation at mid-grid will then take on the order of 10 ns to travel all the way to the grid boundary) and depending on the problem, w ranging from about $0.25\ v_{th}$ up to 3 or $4\ v_{th}$. Figure 3 shows a dip in n near its maximum value for the larger energy group. This dip increases when Δ is reduced and for example, Fig. 4 shows $n(z,t,w)$ and $u(z,t,w)$ for $w = 1.6\ v_{th}$ and for $\Delta = 3$ dx at $t = 2.82$ ns.

Because of this unexpected feature, an exact analytic solution of the model equations, i.e. those including the assumption of an isotropic-microscopic pressure, was sought for that simple case. Noting that each w-group is independent, the equations can be written:

$$\frac{\partial n}{\partial t} + n \frac{\partial u}{\partial z} = 0, \tag{23}$$

$$\frac{\partial u}{\partial t} + \frac{1}{3n} \frac{\partial}{\partial z} \left[n\left(w^2 - u^2\right) \right] = 0. \tag{24}$$

Assuming that a solution of the form

$$u(z,t) = \begin{cases} \dfrac{wz}{R(t)} & z \leq R(t) \\ w & z > R(t) \end{cases} \tag{25}$$

$$n(z,t) = n_i(t) \qquad z \leq R(t) \tag{26}$$

exists, it can be shown that

$$R(t) = \frac{1}{3} wt, \tag{27}$$

and finally the solution for $n(z,t)$ and $u(z,t)$ is obtained:

$$n(z,t) = \begin{cases} n_o t_o^{\,3}/t^3 & 0 < z < \frac{1}{3} wt \\ n_o \left[\dfrac{2wt_o}{3(wt-z)}\right]^3 & \frac{1}{3} wt < z < w\left(t - \frac{2}{3} t_o\right) \\ 0 & w\left(t - \frac{2}{3} t_o\right) < z \end{cases} \tag{28}$$

$$u(z,t) = \begin{cases} 3\ z/t & 0 < z < \frac{1}{3} wt \\ w & \frac{1}{3} wt < z < w\left(t - \frac{2}{3} t_o\right) \\ 0 & w\left(t - \frac{2}{3} t_o\right) < z \end{cases} \tag{29}$$

This solution has been plotted in Fig. 5 and shows a dip in the middle for each and every group w! Thus, even for this most simple problem, the model

equations adopted here (not the numerical implementation) give a poor approximation to the exact solution of the Boltzmann equation, at least for the individual group w. The error turns out to be more than the 20-30% which was thought of as acceptable at the start of this study and a more careful look at the approximation had to be taken.

As indicated before, the only approximation which was made in the model was the assumption of an isotropic-microscopic pressure. To improve the accuracy for the present test problem, we have abandoned this approximation and in its place used a tensor pressure equation. The general form for the pressure tensor equation is

$$\frac{\partial P_{ij}}{\partial t} + \frac{\partial}{\partial x_k}\left(u_k P_{ij}\right) + P_{ik}\frac{\partial u_j}{\partial x_k} + P_{jk}\frac{\partial u_i}{\partial x_k} + \frac{\partial}{\partial x_k} Q_{ijk} + \frac{q}{m} E_k \frac{\partial}{\partial w}\left(\frac{1}{w} u_k P_{ij}\right)$$

$$- \frac{1}{m} B_\ell \left(\varepsilon_{kli} P_{jk} + \varepsilon_{klj} P_{ik}\right) = m\int d^3\underset{\sim}{v}' d^3\underset{\sim}{v}\ \delta(|\underset{\sim}{v}|-w)(v_i-u_i)(v_j-u_j)(K'f'-Kf). \tag{30}$$

To close the moment hierarchy, our next approach is to drop the higher order terms Q that appear now in the equation. Further, using symmetries and properties for the diagonal elements, the original model has been increased by two more equations (in each independent variable) and two more quantities have to be initialized. These are components of the pressure tensor and more calculations have to be performed before starting a problem. However, once all of these steps were accomplished, the original problem was attempted again for a delta-function in space initially (the limiting case of the problem with which the original model had difficulty). Results are shown for $n(z,t,w)$ and $u(z,t,w)$ for $w = 1.6\ v_{th}$ at $t = 3.6$ ns in Fig. 6. We see now that the results are quite acceptable. The model is not quite as simple anymore but the results are much better than the hoped for overall accuracy of 10-30%.

2. Displaced Maxwellian distribution streaming in the direction of motion.

This test problem is very similar to the first one and involves mainly a change in frame of reference. The w-integrated macroscopic density and velocity N and V should be independent of the streaming velocity u except for obvious displacement in z and v_z. However, since the model is not explicitly frame-independent, this test is necessary. The initial distribution function for this case can be written:

$$f(z,v,0) = \frac{C}{\pi^2 v_{th}^2 \Delta} \exp\left(-z^2/\Delta^2\right) \exp\left[-\frac{\left(v_z - u_o\right)^2}{v_{th}^2}\right] \exp\left(-\frac{v_\perp^2}{v_{th}^2}\right). \quad (31)$$

For example, for this case, the microscopic density can be shown to be at all times:

$$n(z,t,w) = \frac{2wC}{\pi v_{th}^3 t} \exp\left[-\frac{w^2 + u_o^2}{v_{th}^2} - \frac{z^2}{\Delta^2} + \frac{t^2}{\Delta^2}\left(\frac{u_o \Delta^2}{v_{th}^2 t^2} + \frac{z}{t}\right)^2\right] \int_{y_1}^{y_2} e^{-y^2} dy,$$

$$\text{with } y_1 = -\frac{t}{\Delta}\left(w + \frac{u_o \Delta^2}{v_{th}^2 t^2} + \frac{z}{t}\right) \text{ and } y_2 = \frac{t}{\Delta}\left(w - \frac{u_o \Delta^2}{v_{th}^2 t^2} - \frac{z}{t}\right). \quad (32)$$

The results for this case depend on the number of energy groups carried in the computation and it was found that twelve groups were needed in order to reproduce reasonably well the macroscopic density and velocity. Figure 7 shows the microscopic density and velocity at t = 3.9 ns for the 11^{th} energy group and the macroscopic density and velocity at the same time. Note that for this problem $P_{xx} \neq 0$ initially but $P_{xy} = 0$. The agreement

for this case is excellent between the analytical and numerical solutions and this change of reference frame due to streaming is not a problem for the model.

3. Displaced Maxwellian distribution streaming in the direction perpendicular to the direction of motion.

Analytically, this case is more complicated than the previous one and for example, both components of the pressure tensor are different from 0 at t = 0. This test problem was originally carried without a pressure tensor formulation. Actually, it was this test, as well as the first test problem (force-free, free-expansion with a localized distribution in space), which showed enough discrepancy with the analytical solution and which forced a re-evaluation of the original model as presented in the second section of this report. Results for this test are shown in Fig. 8 at t = 1 ns both for the macroscopic and microscopic quantities (for the 10^{th} energy group). This calculation was carried out with 12 energy groups again and for $u = 2\ v_{th}$. The agreement between numerical and analytical results is not as good as for the previous case but by comparison with the scalar pressure case formulation, it is a much-needed improvement and is quite satisfactory in view of our criterion for accuracy. The numerical problem which remains seems to be spreading of the macroscopic density, or diffusion, in the z-direction which increases with time. Numerical tests, e.g., changing the number of energy groups did not change the results in any significant way.

4. Shear Flow Problem

Increasing in complexity, we next look at the collision-free shear flow problem characterized by the following initial distribution function f:

$$f(z,v,0) = \frac{C}{\pi^{3/2} v_{th}^3} \exp\left(- \frac{v_x^2 + v_z^2}{v_{th}^2} \right) \exp\left\{ - \frac{\left[v_y - u_o(z) \right]^2}{v_{th}^2} \right\} . \quad (33)$$

Its solution for all times is simply

$$f(z,v,t) = \frac{C}{\pi^{3/2} v_{th}^3} \exp\left\{ - \frac{v_x^2 + v_z^2 + \left[v_y - u_o\left(z - v_z t \right) \right]^2}{v_{th}^2} \right\} , \quad (34)$$

and we consider the special case with the initial condition

$$u_o(z) = \begin{cases} u_o & z > 0 \\ -u_o & z < 0 \end{cases} \quad (35)$$

We can calculate the exact microscopic density and velocity. After some algebra, these quantities can be shown to be:

$$n(z,t,w) = \frac{Cw}{\pi^{1/2} v_{th} u_o} \left\{ \exp\left[- \frac{(w-u_o)^2}{v_{th}^2} \right] - \exp\left[- \frac{(w+u_o)^2}{v_{th}^2} \right] \right\} , \quad (36)$$

$$n(z,t,w) u_y(z,t,w) = \frac{2Cw}{\pi^{3/2} v_{th}^3} e^{-(w^2+u_o^2)/v_{th}^2} \int_{-w}^{\infty} dv_y v_y e^{2u_o v_y / v_{th}^2} \int_{-z/t}^{z/t} \frac{dv_z}{\sqrt{w^2 - v_y^2 - v_z^2}}$$

$$\Theta\left(w^2 - v_y^2 - v_z^2 \right), \quad (37)$$

where Θ is the Heavyside function. The last integral can be simplified further for $z^2 > w^2 t^2$ and is written

$$nu_y = \frac{Cwv_{th}}{2\pi^{1/2}u_o^2}\,[\Theta(-z) - \Theta(z)]\left[e^{-(w+u_o)^2/v_{th}^2}\left(\frac{2u_o w}{v_{th}^2} + 1\right) + e^{-(w-u_o)^2/v_{th}^2}\right.$$

$$\left.\left(\frac{2u_o w}{v_{th}^2} - 1\right)\right]. \tag{38}$$

We see that $n(z,t,w)$ is independent of z and t as it must be and that $u(z,t,w)$ is independent of z and t only when $z > wt$. This is because, if z is positive, no particle with speed w which originated in the region $z < 0$ has yet arrived at z; thus there is as yet no mixing of v values.

The system of model equations can be solved analytically for the present case

$$n(z,t,w) = c^t, \tag{39}$$

$$P_{zz}(z,t,w) = c^t, \tag{40}$$

and can be written

$$\frac{\partial u_y}{\partial t} = -\frac{1}{mn}\frac{\partial P_{yz}}{\partial z}, \tag{41}$$

$$\frac{\partial P_{yz}}{\partial t} = -P_{zz}\frac{\partial u_y}{\partial z}. \tag{42}$$

This reduces to a wave equation

$$\frac{\partial^2 u_y}{\partial t^2} = \frac{P_{zz}}{mn}\frac{\partial^2 u_y}{\partial z^2}, \tag{43}$$

$$\frac{\partial^2 P_{yz}}{\partial t^2} = \frac{P_{zz}}{mn}\frac{\partial^2 P_{yz}}{\partial z^2}, \tag{44}$$

to which the solution is any function of the form:

$$u_y(z,t,w) = u_1\left(z + \sqrt{\frac{P_{zz}}{mn}}\, t\right) + u_2\left(z - \sqrt{\frac{P_{zz}}{mn}}\, t\right). \tag{45}$$

To specify u_1 and u_2, we need initial values of u_y $(z,0,w)$ and $[du(z,t,w)/dt]$ at $t = 0$. These values can be obtained from the analytical solution and after some algebra, it becomes

$$u_y(z,t,w) = \frac{\Theta(z)v_{th}}{\pi^{1/2}u_o^2}\int_o^{w(z/t)} dw\, w\, e^{-(w^2+u_o^2)/v_{th}^2}\left[-\sinh\left(\frac{2u_o w}{v_{th}^2}\right)\right.$$

$$\left. + \frac{2u_o w}{v_{th}^2}\cosh\left(\frac{2u_o w}{v_{th}^2}\right)\right], \tag{46}$$

where $w(z/t)$ is determined by the condition

$$\frac{z^2}{t^2} = c^2(\bar{w}) = \frac{P_{zz}(\bar{w})}{mn} = \frac{v_{th}^4}{u_o^2}\left[\frac{2u_o\bar{w}}{v_{th}^2}\cosh\left(\frac{2u_o\bar{w}}{v_{th}^2}\right) - 1\right]. \tag{47}$$

The results for u_y given by the model are shown in Fig. 9 whereas the analytical solution to the Boltzmann equation is shown in dotted lines on the same figure. Once more, a discrepancy exists between the model solution and the exact analytical solution. So, going back to the approximations made in the model, we note that we had closed the hierarchy by setting Q_{ijk} to 0, on the assumption that the Q_{ijk} terms were third order in deviations from average quantities. But the situation is really more complicated. The difficulty in this shear flow problem originates from the fact that correlations are introduced into Q_{ijk} due to the factor

$\delta(v-w)$, i.e., to the fact that averages are taken only on a spherical surface in v-space, and that these correlations, in some cases, introduce terms into Q_{ijk} that are not third-order. Neglecting these terms then gives an inconsistent truncation of the hierarchy. It can be shown that the Q_{yzz} components should be retained and set equal to

$$Q_{yzz} = -2u_y P_{yy} , \tag{48}$$

so that in 1-D the evolution equation for P_{yz} becomes:

$$\frac{\partial P_{yz}}{\partial t} + \frac{\partial}{\partial z} Q_{yzz} + P_{zz} \frac{\partial u_y}{\partial z} = 0. \tag{49}$$

This requires, in turn, an equation for P_{yy} which can be written:

$$\frac{\partial P_{yy}}{\partial t} + \frac{\partial}{\partial z} Q_{yzz} + P_{yz} \frac{\partial u_y}{\partial z} = 0 . \tag{50}$$

But $Q_{yyz} = 0$ and this simplifies to:

$$\frac{\partial P_{yy}}{\partial t} + 2P_{yz} \frac{\partial u_y}{\partial z} = 0 \tag{51}$$

We have picked up another tensor pressure component in the process, though we are still solving a problem in one-dimensional geometry only. Unfortunately, we are finding that as the complexity of the test problem increases, so too does the complexity of the model needed to get a satisfactory solution. We have also found numerical problems in the shear flow test problem, which also require special treatment. The solution for the shear flow problem for $u = 0.5\ v_{th}$ is shown in Fig. 10 and displays strong oscillatory behavior around $z = 0$ (where the velocity changes its sign abruptly). This behavior was improved by dropping the FCT algorithm for P_{yz} and P_{yy} component equations and replacing it instead by

an upwind modified Lax scheme for these quantities. In order to update these quantities, the operator $\partial u/\partial t$ had to be replaced by

$$u_i^{n+1} = 0.7\, u_i^n + 0.15\, \left(u_{i-1}^n + u_{i+1}^n\right), \tag{52}$$

where n and i are respectively the time and spatial indices. The oscillations disappeared until t = 3 ns at which time they reappeared. Another case was run in which the abrupt velocity profile at t = 0 was replaced by a smoother one of the form

$$u_o(z) = u_o \tanh\,(4z). \tag{53}$$

The value of u was also increased to 1.5 v_{th} and the solution for that case is shown in Fig. 11 at t = 3.9 ns. The velocity profile steepened up in time, trying to simulate the previous case. It still showed some oscillatory behavior near z = 0 at a late time. Also, the solution presented some small asymmetry at later times.

VI. Conclusion

In this report, we have examined on a variety of attempts to implement a scheme to solve the Boltzmann equation using an energy group method. Our first attempt to close the hierarchy of moment equations by using a simple approximation on the microscopic pressure for each energy group did not even hold for the simplest test problem, a force-free, free-expanding Maxwellian distribution function. Tensor component equations had to be added for that problem. Having done so, the next test problems, involving a free-streaming distribution with mean velocity in the direction parallel and/or perpendicular to the spatial coordinate, proved to yield a satisfactory solution.

The next problem which dealt with shear flow required the introduction of an extra equation for the higher order heat flow tensor. Numerical problems also appeared in the treatment of a very sharp transition in velocity. Although some of these problems could have been anticipated to some degree, our present feeling now is that continuing degrees of improvement have to be made in order to resolve more and more complicated problems. Our real interest is in problems that are multi-dimensional spatially, which appear likely to introduce a good deal more complexity into the assumption needed to close the hierarchy. Although all the cases under study were collisionless, and because of that, were more difficult to solve numerically (since no physical smoothing was present in the equations), our confidence in the implementation of the method has not reached a point where the solution can be trusted in untested physical situations. The method, which looked very attractive at the beginning because of its simplicity, has been shown to work for the problems studied after some hard work and after the addition of many "corrective" equations. The next step of applying this method to more spatial dimensions and to more realistic problems has not been pursued for the moment.

Acknowledgment

This work was supported by the Defense Advanced Research Projects Agency.

References

1. R. R. Johnston, R. L. Feinstein and D. A. Keeley, SAI-C-51-PA, 1981. R. R. Johnston et al., SAI-C-73-PA, 1985.
2. R. R. Johnston, B. B. Godfrey et al., SAI-C-73-PA, 1985.
3. S. S. Yu and R. E. Melendez, UCRL-91412, 1983 (unpublished). R. R. Johnston, C. Yee et al., SAI-C-73-PA, 1985.
4. L. C. Pitchford, S. V. O'Neil and J. R. Rumble, Jr., Phys. Rev. A23, 294 (1981).
5. S. S. Yu and R. E. Melendez, UCID-19479 (1982) and UCID-19731 (1983).
6. M. Lampe, "A New Technique for Closure of the Boltzmann Equation", Proc. DARPA/Services Propagation Review, June 1986, Sandia National Laboratory.
7. D. Book and J. Boris, J. Comp. Phys. 11, 38 (1973).

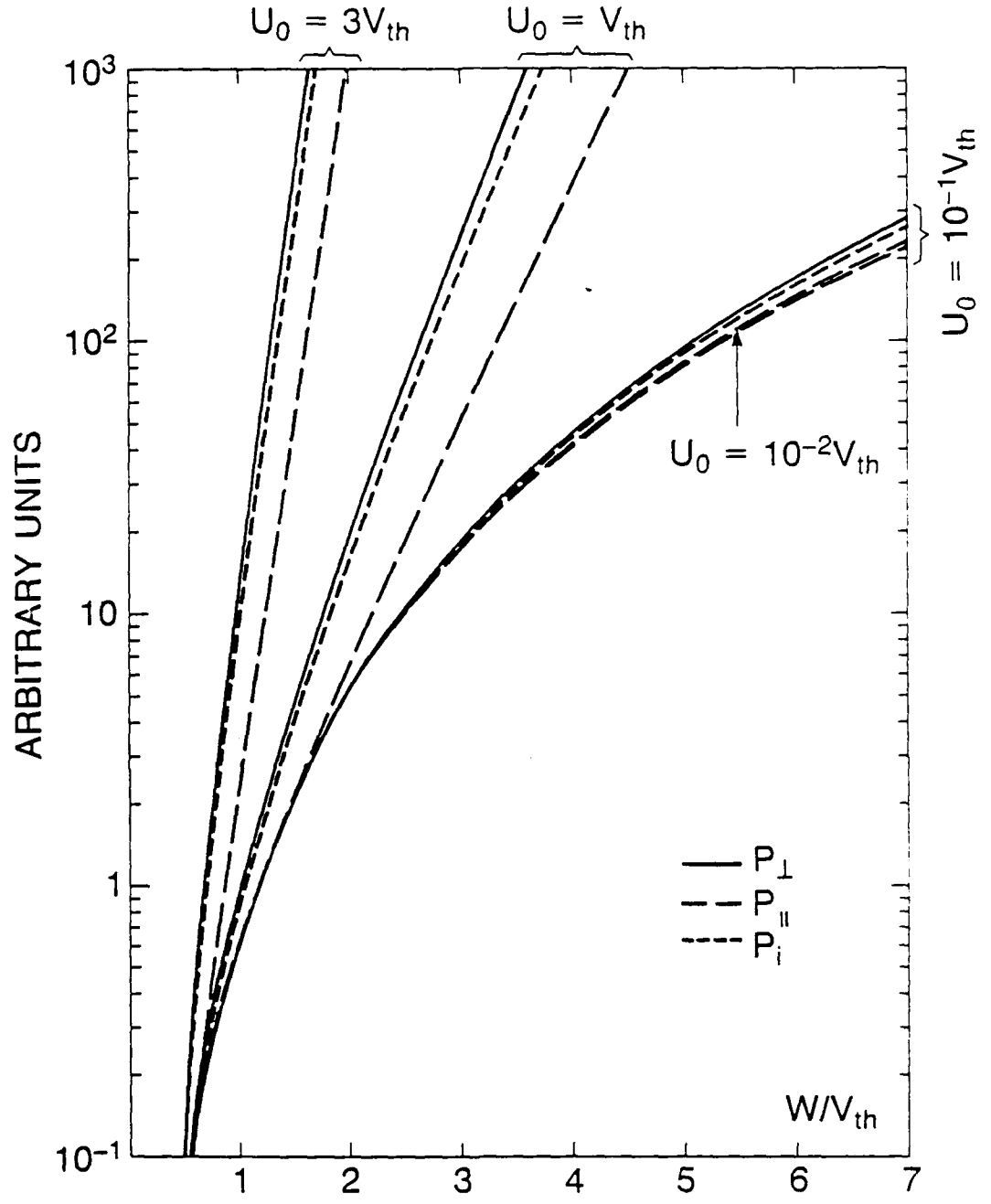

Fig. 1 Comparison between parallel (isotropic) and perpendicular pressure as a function of energy group (w) for various values of u .

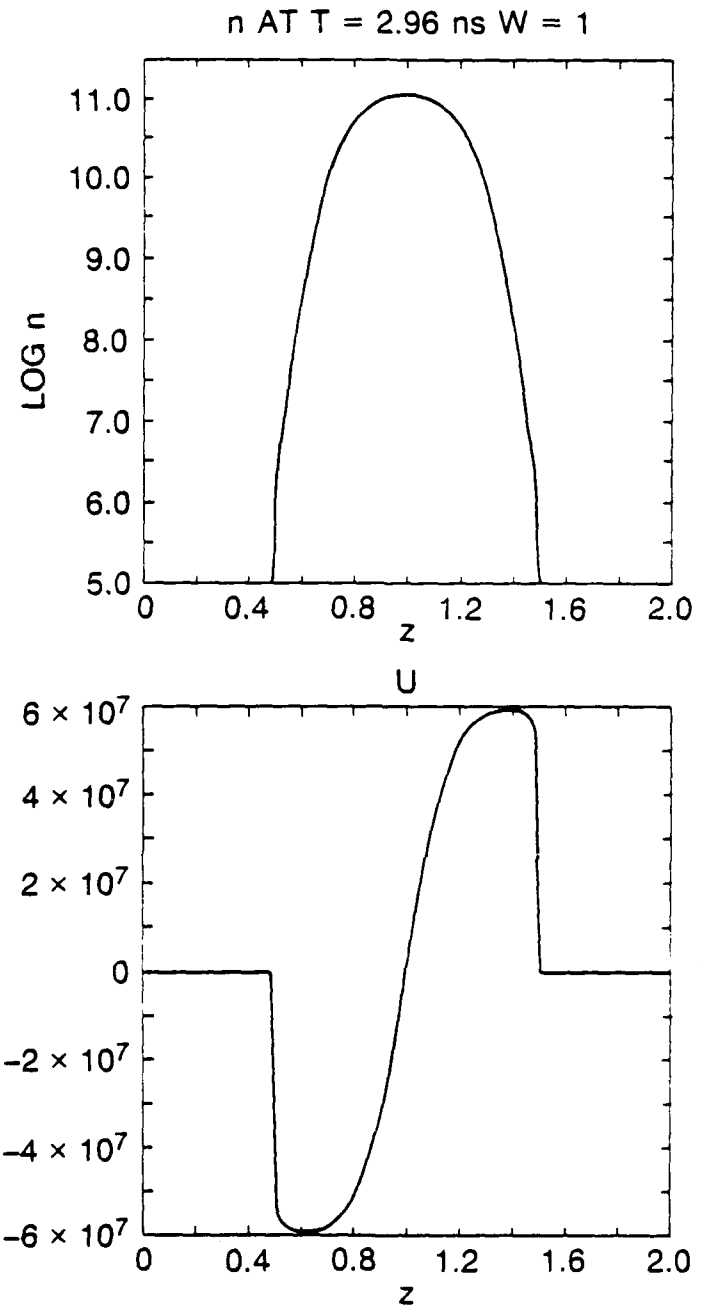

Fig. 2 Microscopic density and velocity for a thin sheet (Δ = 10dx) force-free free-streaming Maxwellian distribution function for $w = 0.6\ v_{th}$ energy group at t = 2.96 ns using an isotropic-microscopic pressure.

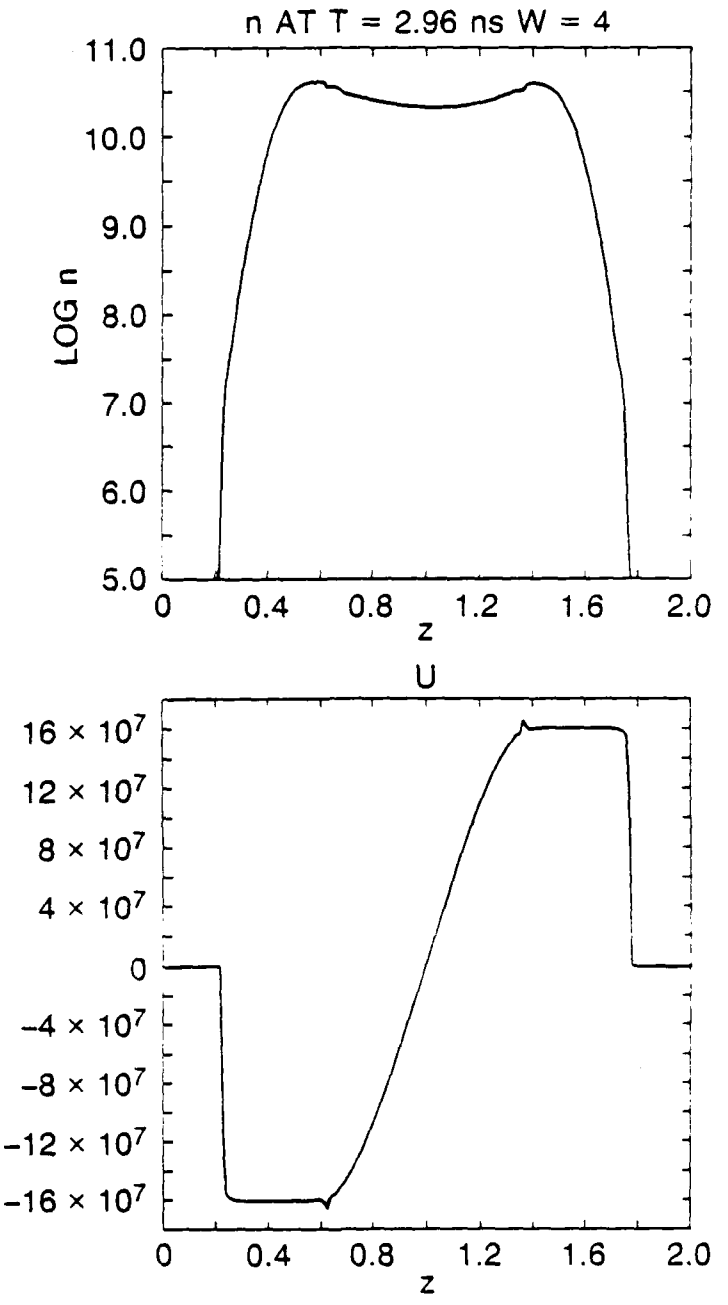

Fig. 3 Same for w = 1.6 v_{th} energy group.

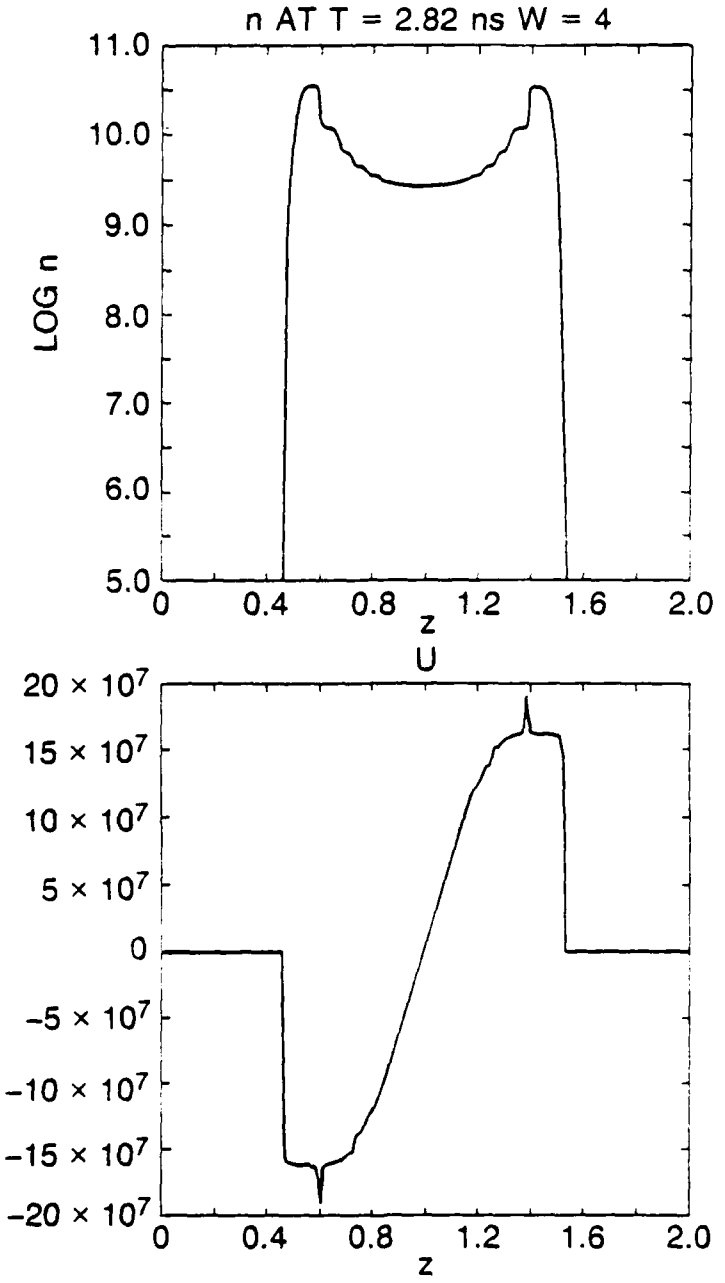

Fig. 4 Same as Fig. 2 for a thinner sheet (Δ = 3 dx) for w = 1.6 v_{th} at t = 2.82 ns.

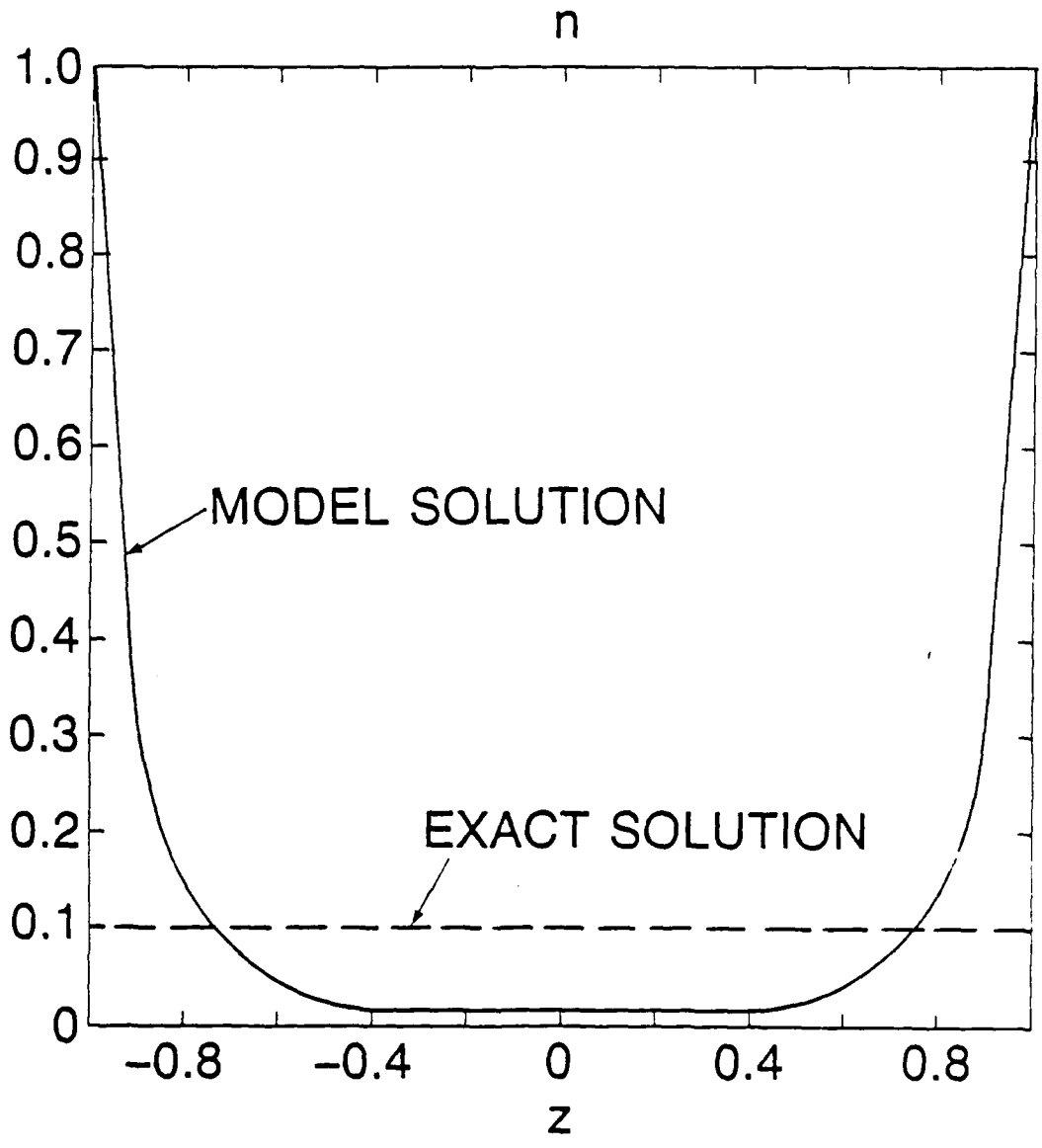

Fig. 5 Dip shown in microscopic density by analytical solution for model equations corresponding to cases of Figs. 2 - 4.

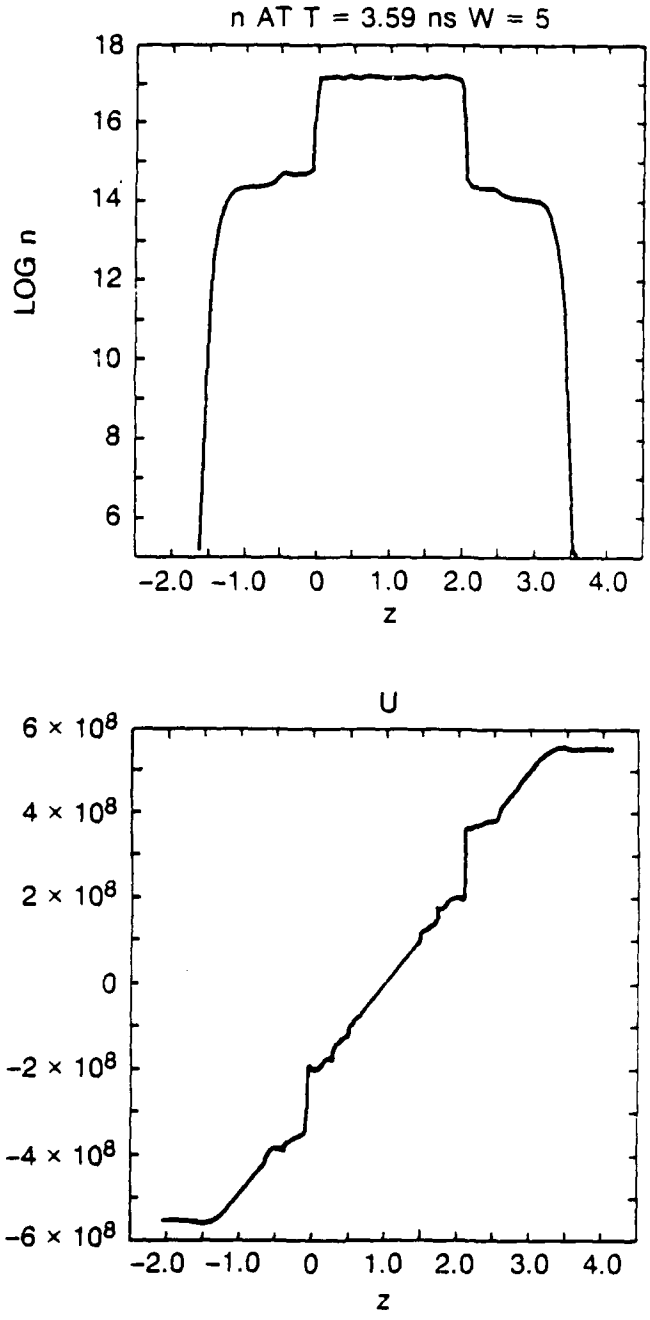

Fig. 6 Microscopic density and velocity for δ-function force-free free-streaming Maxwellian distribution function for $w = 1.6v_{th}$ energy group at t = 3.6 ns using tensor pressure formulation.

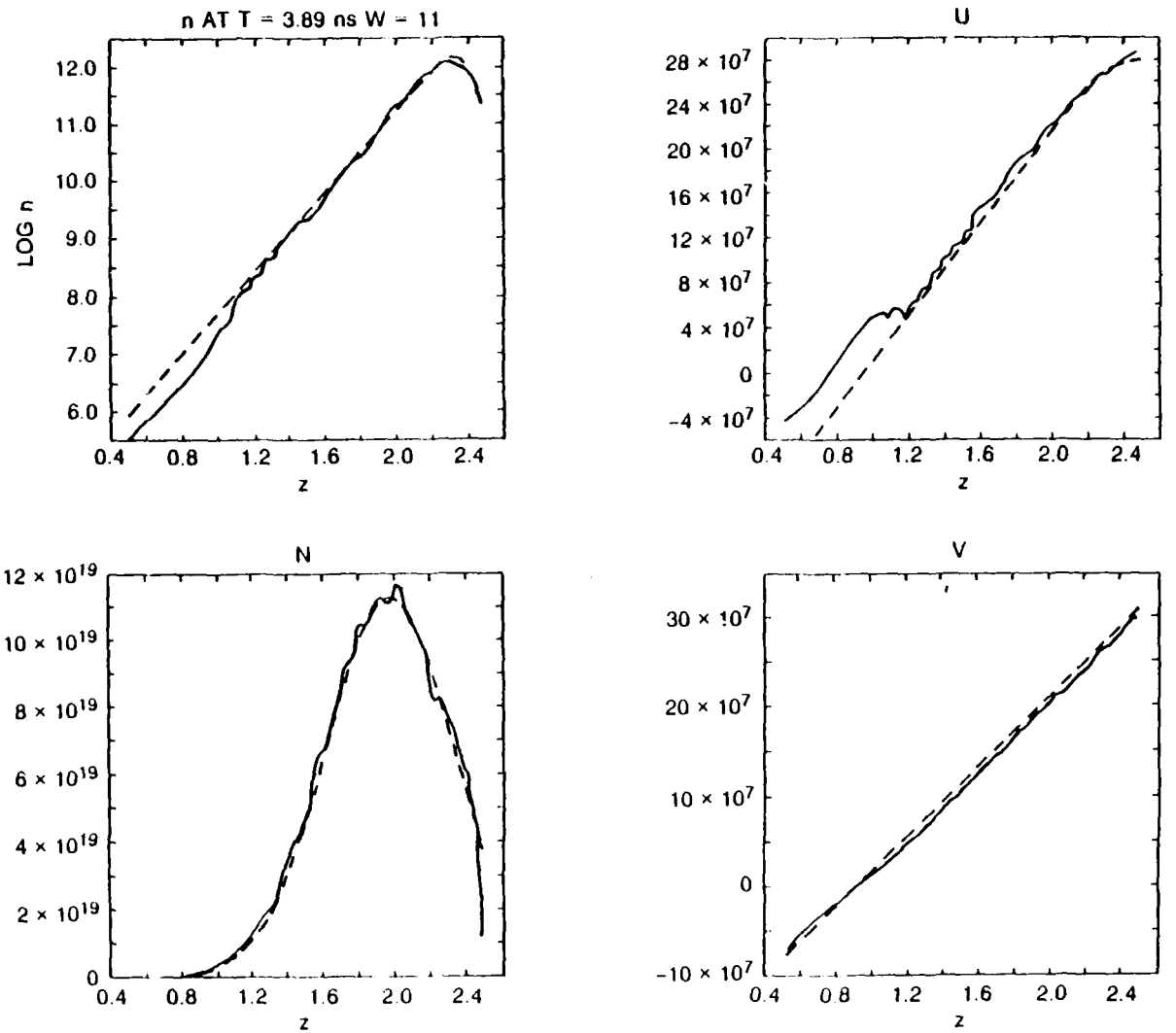

Fig. 7 Microscopic and macroscopic densities and velocities for free-streaming displaced Maxwellian distribution function in the axial direction.

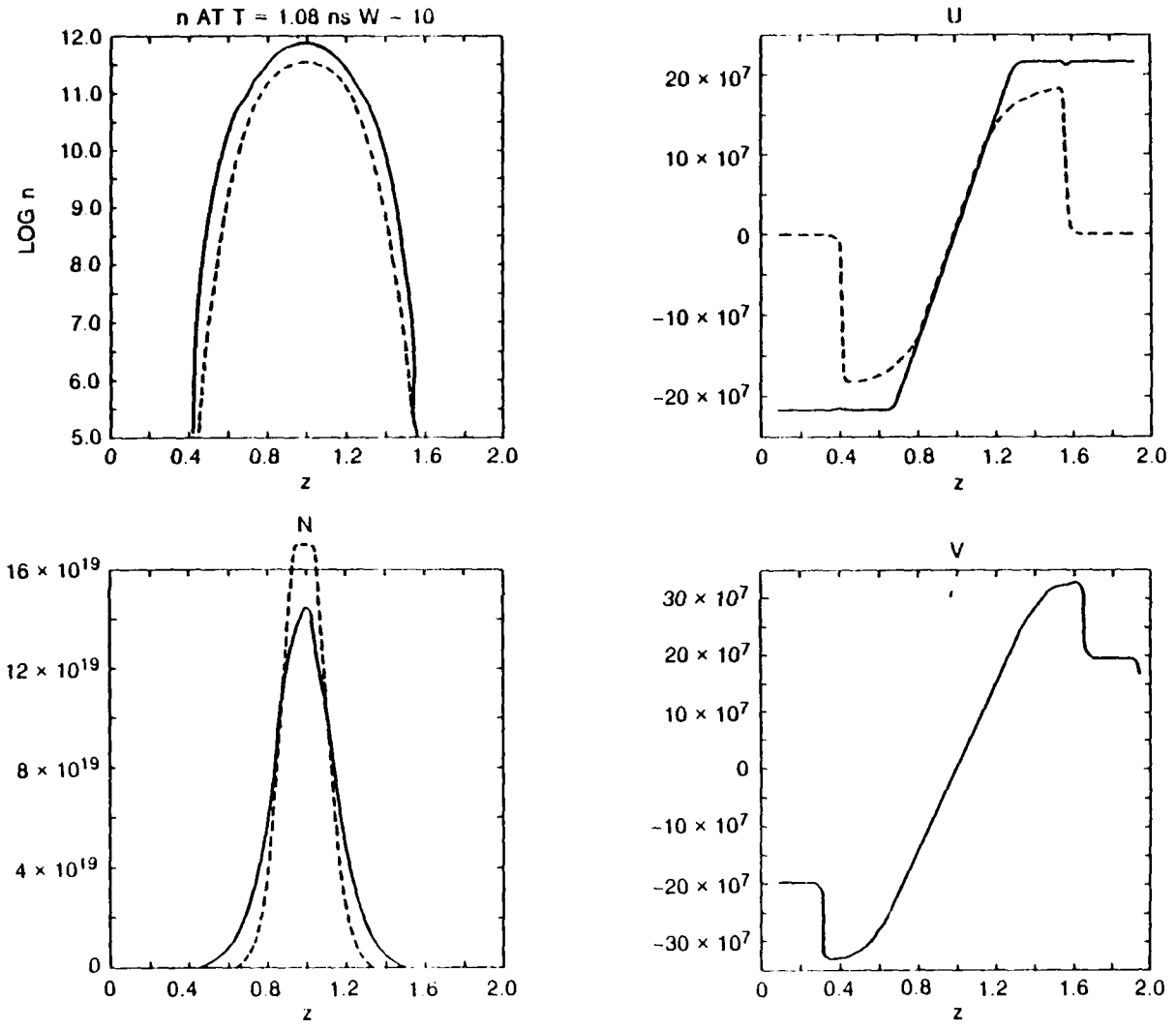

Fig. 8 Same as Fig. 7 for free-streaming Maxwellian distribution function in direction perpendicular to coordinate.

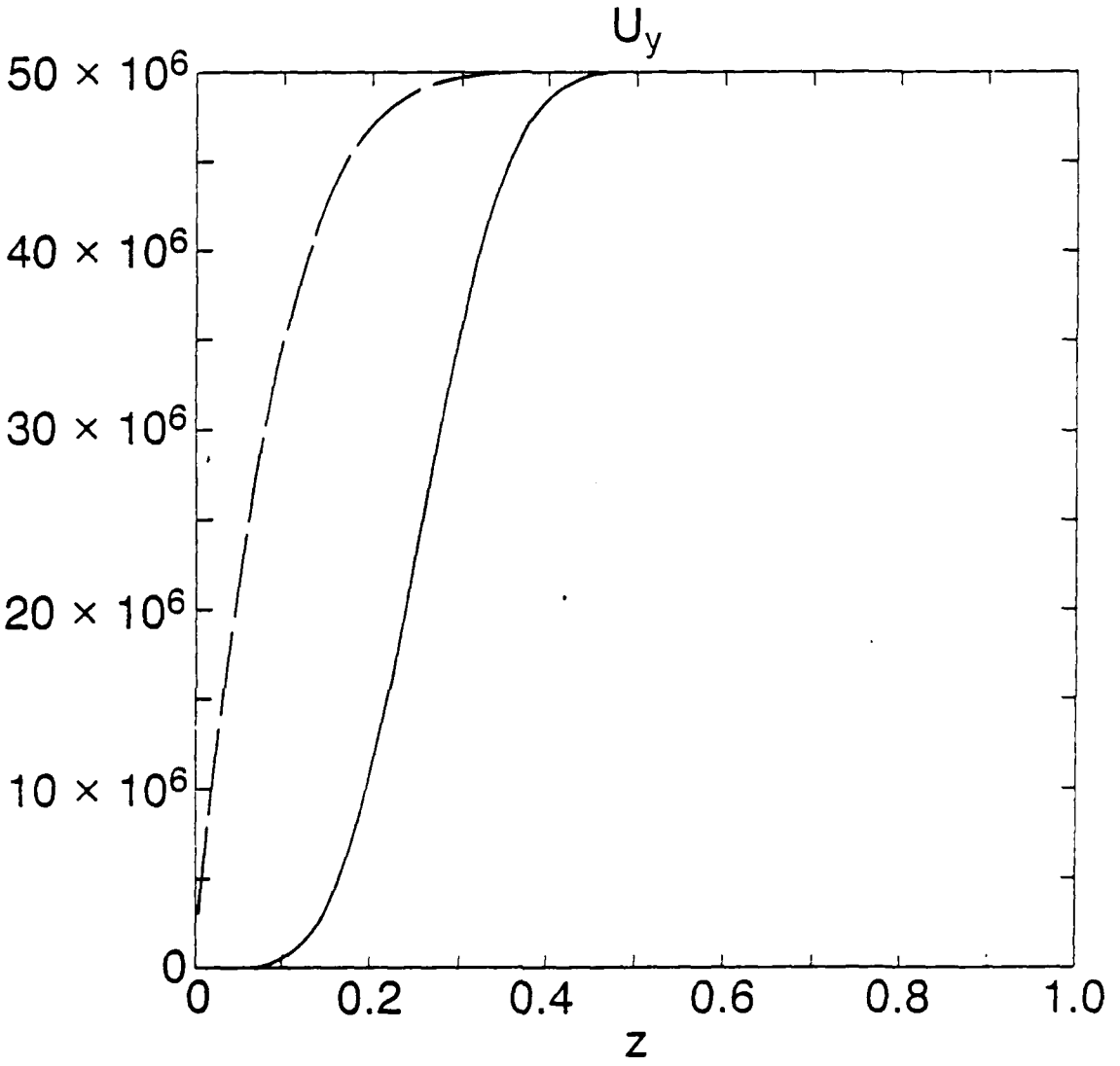

Fig. 9 Model solution for u for shear flow problem at t = 1.6 ns.

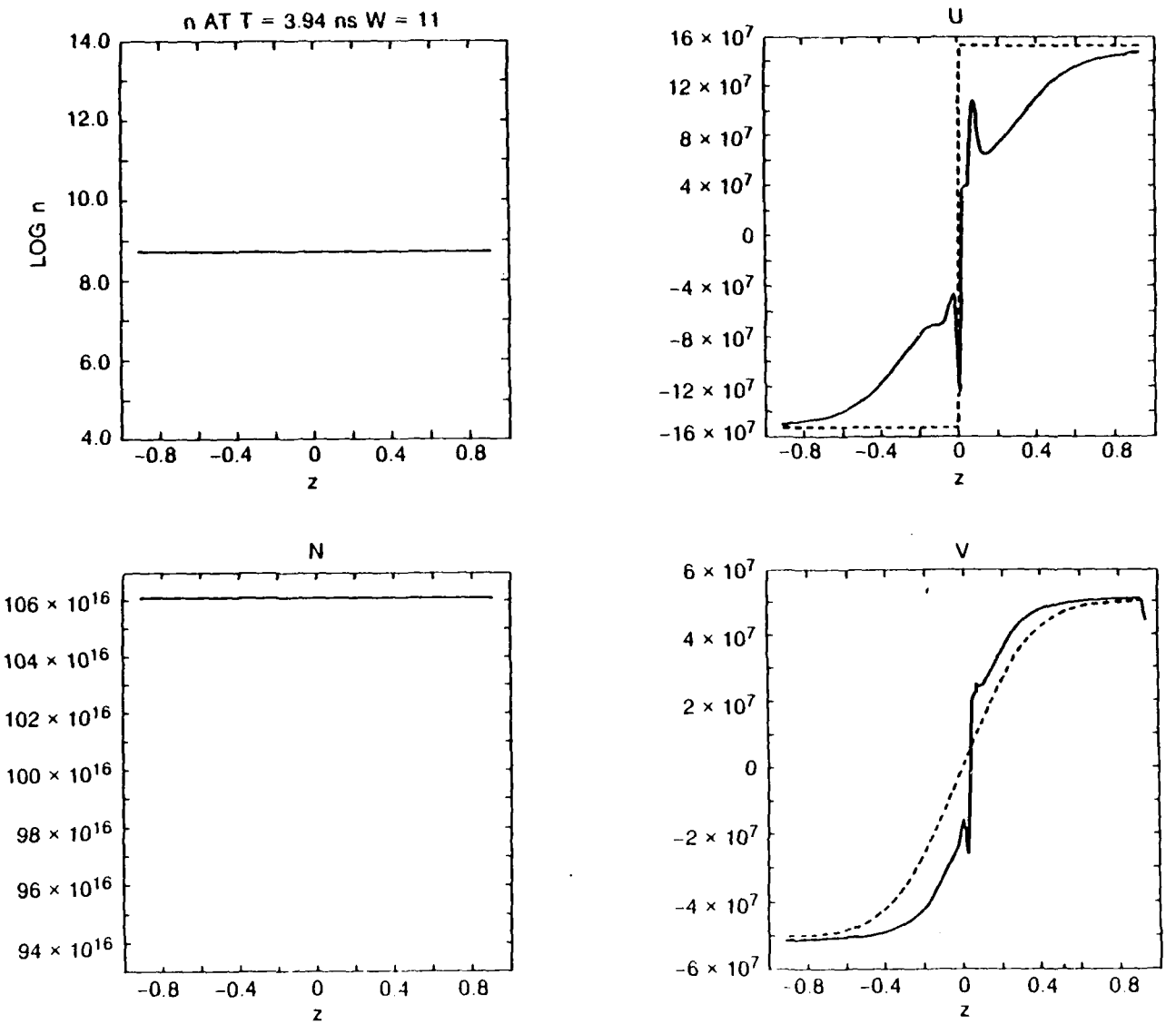

Fig. 10 Microscopic and macroscopic densities and velocities for shear flow problem for sharp velocity transition at z = 0 ($u = 0.5\ v_{th}$) at t = 3.9 ns.

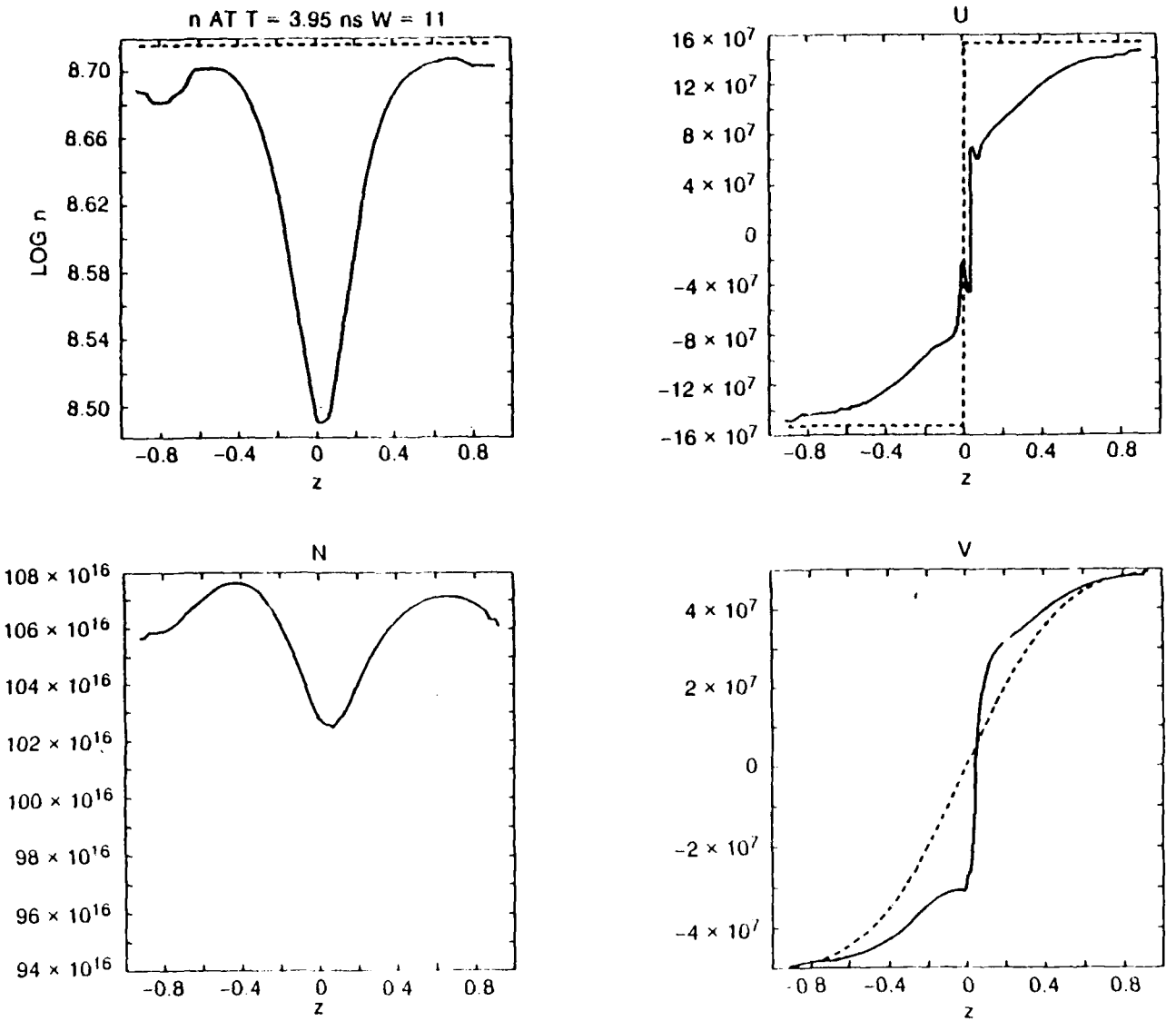

Fig. 11 Same as Fig. 10 for smooth velocity transition at z = 0 (u = 1.5 v_{th}) at t = 3.9 ns.

Distribution List*

Naval Research Laboratory
4555 Overlook Avenue, S.W.
Attn: CAPT J. J. Donegan, Jr. - Code 1000
Dr. M. Lampe - Code 4792 (20 copies)
Dr. T. Coffey - Code 1001
Head, Office of Management & Admin - Code 1005
Deputy Head, Office of Management & Admin - Code 1005.1
Directives Staff, Office of Management & Admin - Code 1005.6
Director of Technical Services - Code 2000
ONR - Code 0124
NRL Historian - Code 2604
Dr. W. Ellis - Code 4000
Dr. J. Boris - Code 4040
Dr. M. Picone - Code 4040
Dr. M. Rosen - Code 4650
Dr. M. Haftel - Code 4665
Dr. S. Ossakow - Code 4700 (26 copies)
Dr. A. Robson - Code 4708
Dr. M. Friedman - Code 4750
Dr. R. Meger - Code 4750
Dr. J. Antoniades - Code 4751
Dr. T. Peyser - Code 4751
Dr. D. Murphy - Code 4751
Dr. R. Pechacek - Code 4750.1
Dr. G. Cooperstein - Code 4770
Dr. A. Ali - Code 4780
Dr. D. Colombant - Code 4790 (25 copies)
Dr. R. Fernsler - Code 4790
Dr. S. Gold - Code 4790
Dr. I. Haber - Code 4790
Dr. R. F. Hubbard - Code 4790
Dr. G. Joyce - Code 4790
Dr. Y. Lau - Code 4790
Dr. S. P. Slinker - Code 4790
Dr. P. Sprangle - Code 4790
Dr. R. Taylor - 4790
Dr. J. Krall - Code 4790
B. Pitcher - Code 4790A
Code 4790 (20 copies)
Mr. P. Boris - SAIC (Code 4790)
Library - Code 2628 (22 copies)
D. Wilbanks - Code 2634
Code 1220

* Every name listed on distribution gets one copy except for those where extra copies are noted.

Air Force Office of Scientific Research
Physical and Geophysical Sciences
Bolling Air Force Base
Washington, DC 20332
Attn: Major Bruce Smith

Air Force Weapons Laboratory
Kirtland Air Force Base
Albuquerque, NM 87117-6008
Attn: W. Baker (AFWL/NTYP)
D. Dietz (AFWL/NTYP)
R. W. Lemke
B. Godfrey

U. S. Army Ballistics Research Laboratory
Aberdeen Proving Ground, Maryland 21005
Attn: Dr. Donald Eccleshall (DRXBR-BM)
Dr. Anand Prakash
Dr. Clinton Hollandsworth

Avco Everett Research Laboratory
2385 Revere Beach Pkwy
Everett, Massachusetts 02149
Attn: Dr. R. Patrick
Dr. Dennis Reilly

Ballistic Missile Def. Ad. Tech. Ctr.
P.O. Box 1500
Huntsville, Alabama 35807
Attn: Dr. M. Hawie (BMDSATC-1)

Chief of Naval Material
Office of Naval Technology
MAT-0712, Room 503
800 North Quincy Street
Arlington, VA 22217
Attn: Dr. Eli Zimet

Commander
Space and Naval Warfare Systems Command
National Center 1, Room 8E08
Washington, DC 20363-5100
Attn: RADM Robert L. Topping

Cornell University
369 Upson Hall
Ithaca, NY 14853
Attn: Prof. David Hammer

DASIAC - DETIR
Kaman Tempo
25600 Huntington Avenue, Suite 500
Alexandria, VA 22303
Attn: Mr. F. Wimenitz

Defense Advanced Research Projects Agen
1400 Wilson Blvd.
Arlington, VA 22209
Attn: Dr. H. L. Buchanan
Dr. B. Hui

Defense Nuclear Agency
Washington, DC 20305
Attn: Dr. Muhammad Owais (RAAE)

Department of Energy
Washington, DC 20545
Attn: Dr. Wilmot Hess (ER20:GTN,
High Energy and Nuclear Physics)
Mr. Gerald J. Peters (G-256)

Directed Technologies, Inc.
1500 Wilson Blvd. Suite 515
Arlington, VA 22209
Attn: Mr. Ira F. Kuhn
Dr. Nancy Chesser

C. S. Draper Laboratories
555 Technology Square
Cambridge, Massachusetts 02139
Attn: Dr. E. Olsson

General Dynamics Corporation
Pomana Division
1675 W. Mission Blvd.
P. O. Box 2507
Pomana, CA 92769-2507
Attn: Dr. Ken W. Hawko

Hy-Tech Research Corp.
P. O. Box 3422 FSS
Radford, VA 24143
Attn: Dr. Edward Yadlowsky

HQ Foreign Technology Division
Wright-Patterson AFB, OH 45433
Attn: TUTD/Dr. C. Joseph Butler

Institute for Defense Analyses
1801 N. Beauregard Street
Alexandria, VA 22311
Attn: Dr. Deborah Levin
Ms. M. Smith

Intelcom Rad Tech.
P.O. Box 81087
San Diego, California 92138
Attn: Dr. W. Selph

JAYCOR
11011 Torreyana Road
P. O. Box 85154
San Diego, CA 92138-9259
Attn: Dr. Franklin S. Felber
Dr. Seung Kai Wong

JAYCOR
39650 Libery Street, Suite 320
Freemont, CA 9453[illegible]
Attn: Dr. Kendal Casey

Joint Institute for Laboratory Astrophysics
National Bureau of Standards and University of Colorado
Boulder, CO 80309
Attn: Dr. Arthur V. Phelps

Kaman Sciences
1500 Garden of the Gods Road
Colorado Springs, CO 80933
Attn: Dr. John P. Jackson

Kaman Sciences
P. O. Drawer QQ
Santa Barbara, CA 93102
Attn: Dr. W. Hobbs

La Jolla Institute
P. O. Box 1434
La Jolla, CA 92038
Attn: Dr. K. Brueckner

Lawrence Berkeley Laboratory
University of California
Berkeley, CA 94720
Attn: Dr. Edward P. Lee
Dr. Thomas Fessenden

Lawrence Livermore National Laboratory
University of California
Livermore, California 94550
Attn: Dr. Simon S. Yu
Dr. Frank Chambers
Dr. James W.-K. Mark, L-477
Dr. William Fawley
Dr. William Barletta
Dr. William Sharp
Dr. Daniel S. Prono
Dr. John K. Boyd
Dr. John Clark
Dr. George J. Caporaso
Dr. Donald Prosnitz
Dr. John Stewart
Dr. Y. P. Chong
Major Kenneth Dreyer
Dr. Hans Kruger
Dr. Thaddeus J. Orzechowski
Dr. Michael R. Teague
Mr. John T. Weir

Dr. James E. Leiss
13013 Chestnut Oak Drive
Gaithersburg, MD 20878

Lockheed Missiles and Space Co.
3251 Hanover St.
Bldg. 205, Dept 92-20
Palo Alto, CA 94304
Attn: Dr. John Siambis

Los Alamos National Laboratory
P.O. Box 1663
Los Alamos, NM 87545
Attn: Dr. L. Thode
Dr. H. Dogliani, MS-5000
Mr. R. Carlson, MS-P940
Dr. Carl Ekdahl, MS-D410
Dr. Joseph Mack
Dr. Melvin I. Buchwald
Dr. David C. Moir

Maxwell Laboratories Inc.
8888 Balboa Avenue
San Diego, CA 92123
Attn: Dr. Ken Whitham

McDonnell Douglas Research Laboratories
Dept. 223, Bldg. 33, Level 45
Box 516
St. Louis, MO 63166
Attn: Dr. Carl Leader
Dr. Frank Bieniosek
Dr. John Honig

Mission Research Corporation
1720 Randolph Road, S.E.
Albuquerque, NM 87106
Attn: Dr. Thomas Hughes
Dr. Lawrence Wright
Dr. Kenneth Struve
Dr. Michael Mostrom
Dr. Dale Welch

Mission Research Corporation
P. O. Drawer 719
Santa Barbara, California 93102
Attn: Dr. C. Longmire
Dr. N. Carron

National Bureau of Standards
Gaithersburg, Maryland 20760
Attn: Dr. Mark Wilson

Naval Postgraduate School
Physics Department (Code 61)
Monterey, CA 93940
Attn: Prof. John R. Neighbours
Prof. Fred Buskirk
Prof. Kai Woehler
Prof. Xavier Maruyama

Naval Surface Warfare Center
White Oak Laboratory
Code R-41
Silver Spring, Maryland 20903-5000
Attn: Mr. W. M. Hinckley
Dr. M. H. Cha
Dr. H. S. Uhm
Dr. R. Fiorito
Dr. K. T. Nguyen
Dr. R. Stark
Dr. H. C. Chen
Dr. D. Rule
Dr. Matt Brown
Mrs. Carolyn Fisher (G42)
Dr. Eugene E. Nolting (H23)

Office of Naval Research
800 North Quincy Street
Arlington, VA 22217
Attn: Dr. C. W. Roberson
Dr. F. Saalfeld

Office of Naval Research (2 copies)
Department of the Navy
Code 01231C
Arlington, VA 22217

Office of Under Secretary of Defense
Research and Engineering
Room 3E1034
The Pentagon
Washington, DC 20301
Attn: Dr. John MacCallum

Physics International, Inc.
2700 Merced Street
San Leandro, CA. 94577
Attn: Dr. E. Goldman
Dr. James Benford
Dr. George B. Frazier
Mr. Ralph Genuario

Princeton University
Plasma Physics Laboratory
Princeton, NJ 08540
Attn: Dr. Francis Perkins, Jr.

Pulse Sciences, Inc.
600 McCormack Street
San Leandro, CA 94577
Attn: Dr. Sidney Putnam

Pulse Sciences, Inc.
2001 Wilshire Boulevard
Suite 600
Santa Monica, CA 90403
Attn: Dr. John R. Bayless
Dr. R. Adler

The Rand Corporation
2100 M Street, NW
Washington, DC 20037
Attn: Dr. Nikita Wells
Mr. Simon Kassel

Sandia National Laboratory
Albuquerque, NM 87115
Attn: Dr. David Hasti/1272
Dr. Collins Clark
Dr. John Freeman/1241
Dr. Charles Frost
Dr. George Kamin/1274
Dr. Gordon T. Leifeste
Dr. Gerald N. Hays
Dr. Michael G. Mazarakis/1272
Dr. John Wagner/1241
Dr. Ron Lipinski/1274
Dr. James Poukey
Dr. Milton J. Clauser/1261
Dr. Kenneth R. Prestwich/1240
Dr. Kevin O'Brien
Dr. Isaac R. Shokair
Dr. J. Pace VanDevender/1200

Science Applications Intl. Corp.
5150 El Camino Road
Los Altos, CA 94022
Attn: Dr. R. R. Johnston
Dr. Leon Feinstein
Dr. Douglas Keeley
Dr. E. Roland Parkinson

Science Applications Intl. Corp.
1710 Goodridge Drive
McLean, VA 22102
Attn: Mr. W. Chadsey
Dr. A Drobot
Dr. K. Papadopoulos
Dr. William W. Rienstra
Dr. Alan J. Toepfer
Dr. Alfred Mondelli
Dr. D. Chernin
Dr. R. Tsang

Science Research Laboratory, Inc.
1600 Wilson Boulevard
Suite 1200
Arlington, VA 22209
Attn: Dr. Joseph Mangano
Dr. Daniel Birx

Commander
Space & Naval Warfare Systems Command
PMW-145
Washington, DC 20363-5100
Attn: CAPT J. D. Fontana
LT Fritchie

SRI International
PS0-15
Molecular Physics Laboratory
333 Ravenswood Avenue
Menlo Park, CA 94025
Attn: Dr. Donald Eckstrom
Dr. Kenneth R. Stalder

Strategic Defense Initiative Org.
SDIO/T/DEO
The Pentagon
Washington, DC 20009-7100
Attn: Lt Col R. L. Gullickson
Dr. D. Duston

Titan/Spectron, Inc.
P. O. Box 4399
Albuquerque, NM 87196
Attn: Dr. R. Bruce Miller
Dr. John Smith

Titan Systems, Inc.
2685 Marine Way
Suite 1408
Mountain View, CA 94043
Attn: Dr. Kenneth W. Billman

Titan Systems, Inc.
9191 Towne Centre Dr.-Suite 500
San Diego, CA 92122
Attn: Dr. R. M. Dowe

University of California
Physics Department
Irvine, CA 92664
Attn: Dr. Gregory Benford
Dr. Norman Rostoker

University of California
San Diego, CA 92110
Attn: Dr. Marshall N. Rosenbluth

University of Maryland
Physics Department
College Park, MD 20742
Attn: Dr. Y. C. Lee
Dr. C. Grebogi
Dr. W. Destler
Dr. C. Striffler

University of Michigan
Dept. of Nuclear Engineering
Ann Arbor, MI 48109
Attn: Prof. Terry Kammash
Prof. R. Gilgenbach

Director of Research
U.S. Naval Academy
Annapolis, MD 21402 (2 copies)

Do NOT make labels
for these two-below:
Records---(1 copy)

Naval Research Laboratory
Washington, DC 20375-5000
Code 2630
Timothy Calderwood